ELSEVIER

International Journal of Solids and Structures 40 (2003) 7299–7314

INTERNATIONAL JOURNAL OF SOLIDS and STRUCTURES

www.elsevier.com/locate/ijsolstr

Predicting the creep lives of thin-walled cylindrical polymeric pipe linings subject to external pressure

J.C. Boot *, I.L. Toropova, A.A. Javadi

School of Engineering, Design and Technology, University of Bradford, Richmond Road, Bradford BD9 6HR, UK

Received 4 August 2003; received in revised form 4 August 2003

Abstract

Installation of a close-fitting polymeric thin-walled lining is now standard practice for the rehabilitation of deteriorating gravity pipes. Design of these linings focuses primarily on their ability to resist an external head of groundwater pressure whilst experiencing long-term creep deformations. Existing structural design guidelines are crude and do not provide consistent safety factors. In this paper an existing simple analysis for linear elastic (geometrically non-linear) buckling loads is developed into a time stepping procedure for calculation of the creep lives of time dependent non-linearly elastic systems subject to long-term constant pressure. The results so obtained using different simulations of the creep data obtained for a particular material are then compared with those derived from a set of corresponding physical tests and alternative numerical modelling, and appropriate conclusions are drawn.

Keywords: Pipe; Lining; Creep; Analysis; Viscoelasticity; Design

1. Introduction

Polymeric pipe linings are now routinely used to renovate deteriorating gas, water, and sewerage pipes. In the latter case the pipes run under low flow conditions except during occasional periods of peak loading and are hydraulically designed to ensure gravity flow under normal conditions. Deterioration of a sewer (gravity) pipe is normally initiated by internal durability problems, and takes the form of a regular pattern of longitudinal cracks (WRc Engineering, 1995). Groundwater then starts to wash the soil support into the pipe, leading to gradual loss of shape and consequent reduction in load carrying capacity of the soil–pipe system. Nevertheless, provided hydraulic integrity of the system can be restored at small deformations (i.e., in a state of stable equilibrium) the original system remains capable of carrying all superimposed ground and traffic loading (Gumbel, 1997; Boot et al., 2001). This is the situation achieved by installation of a close-fitting, thin-walled (i.e., low stiffness), impermeable, polymeric lining. The lining does not bond to the host pipe, and therefore does not form a composite structure with it (WRc Engineering, 1995). The lining is

* Corresponding author. Tel.: +44-1274-233845; fax: +44-1274-234158.
E-mail address: j.c.boot@bradford.ac.uk (J.C. Boot).

0020-7683/$ - see front matter © 2003 Elsevier Ltd. All rights reserved.
doi:10.1016/S0020-7683(03)00440-2

therefore only required to sustain the head of hydrostatic pressure that must be assumed to build up, and be transferred though the cracked pipe, once hydraulic integrity is ensured. This paper focuses attention on the structural behaviour of such linings installed in pipes of nominally cylindrical geometry, as this is the most common situation in practice.

All the current generation thermoset and thermoplastic materials used for pipes and pipe linings are amorphous polymers; they can be assumed to behave in a linear elastic manner under short-term loading below a threshold stress, but always exhibit creep under sustained loading (Struik, 1978). Due to the groundwater pressure acting in the annulus between the host pipe and lining, and the effectively rigid constraint provided by the host pipe, the lining will be subject to a state of combined bending and direct thrust in the plane of the cross-section, which can normally be assumed to be under plane strain or plain stress (Boot and Javadi, 1998b) conditions. In the case of thin-walled linings with nominally circular cross-section, the compressive stresses can reach a relatively high level (in comparison to an unconstrained pipe), and consequently flexural creep will cause progressively increasing axial–flexural interaction. Providing an adequate factor of safety against constrained creep buckling (within the confines of the host pipe, and over a specified minimum design life) therefore constitutes the prime design criterion for these linings (Yamamoto and Matsubara, 1981; Boot and Welch, 1996; Toropova and Boot, 1998).

The first significant study of the buckling capacity of thin-walled cylindrical linings was undertaken by Amstutz (1969), who considered the elastic buckling of steel linings for concrete pipes and pressure vessels, and included both flexural and axial deformations in his analysis, together with the dominant non-linear term in the latter. Boot and Welch (1996) developed a fully consistent finite element (FE) analysis capable of incorporating all essential features of nominally cylindrical polymeric linings, including the effects of imperfect geometry and visco-elastic material behaviour. However, this approach is not suitable for routine design due to its lack of portability, and the cost of maintaining a commercial FE package for a low cost pipe renovation technique. A simplified but consistent procedure, capable of incorporating all the essential features of the system, is required.

Glock (1977) reformulated Amstutz's elastic analysis and obtained a convenient closed form solution for the case of perfectly cylindrical systems assuming the lining adopts a single lobe mode of deformation. Glock's analysis has recently been used as the basis for obtaining buckling pressures for a particular type of commercially available polymeric sewer lining subject to increasing short-term loading to failure (Omara et al., 1997). To allow for the effects of imperfections in real systems, they also introduced an empirical coefficient based on their physical testing results. El-Sawy and Moore (1997) and Moore (1998) have similarly attempted to obtain an imperfection parameter to include in Glock's analysis by using FE analysis. However, Boot (1998) has shown how Glock's analysis can be consistently re-expressed to include the effect of a small annular imperfection between the perfectly circular lining and rigid frictionless constraining boundary simulating the host pipe. This shows that two independent parameters are required to correctly model the effects of varying gap. Furthermore, lined gravity pipe systems can incorporate variable magnitudes of several different types of imperfection, and can deform into one or two lobe modes dependent on whether the imperfect system is predominantly symmetrical or asymmetrical (Boot, 1998; Gumbel, 2001). It is inevitable therefore that a single empirically obtained imperfection coefficient, applied to a particular deformation mode, cannot be used to provide a consistent design safety factor to the full range of systems requiring specification. In addition the theoretical treatments so far discussed do not address the material creep aspect of practical field systems.

Current design criteria for polymeric pipe linings subject to external pressure (WRc Engineering, 1995; ASTM, 1998) use a modified version of the classical linear elastic buckling solution for an unrestrained cylinder (Guice et al., 1994). A (secant) modulus, appropriately reduced from the short-term value, is incorporated to obtain a correspondingly reduced *elastic* buckling load to simulate creep buckling behaviour. The poor simulation of the effects of geometry this implies (Boot and Javadi, 1998a,b) can be significantly enhanced by utilising Glock's analysis in the same manner (Omara et al., 1997). However, the theoretical

validity of obtaining an equivalent buckling load in this way is verified only for the case of steady state creep (Hult, 1966), which depends on linear strain–displacement relationships to maintain the strains at all points at the same relative magnitudes throughout the deformation process. In addition the reduced modulus specified for industrial applications (WIS 4-34-04, 1995) is the 50 year modulus obtained in flexure at a particular stress level, and this may not be representative of the actual behaviour of field systems which are subject to a combination of axial compression and flexural deformations.

What is required therefore is a simple theoretical analysis which can allow for the non-linear effects of geometry and variable imperfection modes, and which provides a consistent simulation of the actual material properties. Accordingly, in this paper Boot's analysis (1998) for the geometrically non-linear buckling of a linearly elastic ring, subject to an annular imperfection, is re-worked to make a consistent allowance for the observed creep behaviour. The results so obtained are compared with the available physical test results, and FE analysis incorporating the same material information, and appropriate conclusions are drawn.

2. Formulation of the basic system equations

If a lining is installed at a very close fit within a perfectly cylindrical host pipe, such as is the case (ASTM, 1998) when the lining is installed as a cured-in-place pipe (CIPP), then surface roughness and differential temperature movements tend to be the dominant sources of geometric imperfections. Under these circumstances the overall observed initial imperfection mode tends to take the form of a small symmetric gap (Guice et al., 1994) as shown in Fig. 1a, and attention can be focused on any representative (e.g., unit) length of lining. The system has radius R (taken as the mean lining radius) and a small symmetrical lack of fit given by:

$$w_0 = w_{02} \tag{1a}$$

When subject to external pressure, system symmetry results in the two lobe mode of deformation illustrated in Fig. 1b. Fig. 2a illustrates the loose fit situation normally achieved when a factory-produced lining pipe is winched into the host pipe (see e.g., Weaver et al., 1999). The asymmetrical lack of fit can now be written as Boot (1998):

$$w_0(\Phi) = w_{01}\left(1 - \frac{\Phi}{\pi}\right) \tag{1b}$$

where w_{01} is the maximum lack of fit, and ϕ is the central angle measured from the position of w_{01} (see Figs. 2 and 3a). When subject to external pressure, the lining will now deform in the single lobe mode illustrated

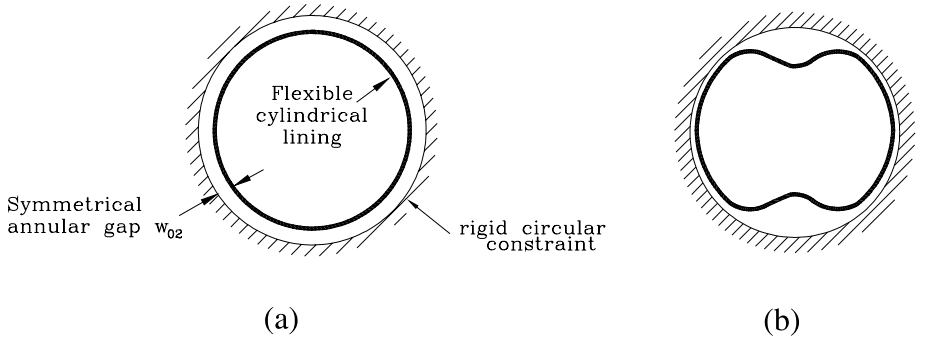

Fig. 1. Close fit lining: (a) undeformed and (b) deformed lining.

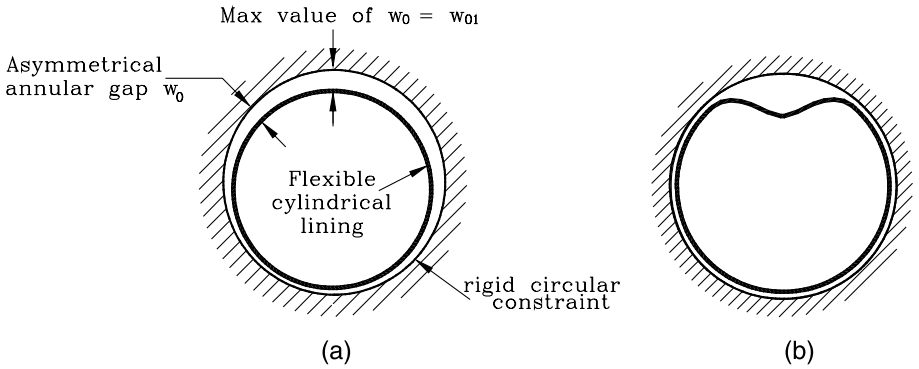

Fig. 2. Loose fit lining: (a) undeformed and (b) deformed lining.

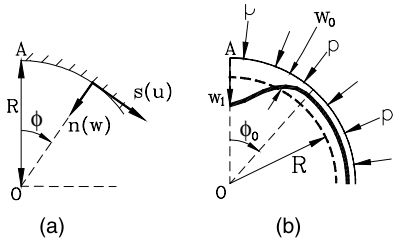

Fig. 3. Basic geometry considered for two lobe deformation: (a) definition of coordinate systems and displacement components and (b) definition of initial and deformed lining geometries.

in Fig. 2b, with w_1 the maximum lobe deformation, and $2\phi_0$ the angle subtended by the lobe at the centre of the pipe (see Fig. 3b).

Consider the deformation modes delineated in Figs. 1b and 2b caused by application of the annulus pressure. The shape of the deformed lobe can be expressed in the form (Glock, 1977; Boot, 1998):

$$w(\Phi) = w_1 \cos^2\left(\frac{\pi\Phi}{2\Phi_0}\right) \tag{2}$$

Under the conditions of interest here the fully non-linear axial membrane strains (ε) and bending strains (κ) can be reduced to (Omara et al., 1997):

$$\varepsilon = \frac{w - w_0}{R} - \frac{\partial u}{\partial s} - \frac{1}{2}\left(\frac{\partial(w - w_0)}{\partial s}\right)^2 \tag{3a}$$

$$\kappa = \frac{(w - w_0)}{R^2} + \frac{\partial^2(w - w_0)}{\partial s^2} \tag{3b}$$

For isotropic linear elastic behaviour the corresponding axial forces and bending moments per unit length of lining are then given by:

$$N = E \cdot A \cdot \varepsilon; \quad M = E \cdot I \cdot \kappa \tag{4a,b}$$

where E is the elastic modulus of the lining material, A and I are the area and second moment of area respectively of the lining per unit length of pipe, and plane stress conditions are assumed in the lining; for plane strain conditions in the lining E is replaced by $E/(1 - \nu^2)$.

Then for small deformation behaviour, the stress can be assumed constant over a strain increment, and the principle of stationary potential energy (Washizu, 1982) can be written for a lining ring of unit length:

$$\delta\Pi_p = \int_0^{\pi D} N\,\delta\varepsilon\,\mathrm{d}s + \int_0^{\pi D} M\,\delta\kappa\,\mathrm{d}s - \int_0^{\pi D} p\,\delta w = 0 \tag{5}$$

where $D = 2R$ and $\mathrm{d}s = R\mathrm{d}\phi$.

Substituting Eqs. (1–4) into Eq. (5) and rearranging yields:

$$f_1 = \frac{\pi}{8}\frac{EI}{R^3}\left(\frac{\pi}{\phi_0}\right)^3 w_1 + 2CN\frac{\partial N}{\partial w_1} - p\phi_0\frac{R}{2} = 0 \tag{6}$$

$$f_2 = -\frac{3}{16}\frac{EI}{R^3}\left(\frac{\pi}{\phi_0}\right)^4 w_1^2 + 2CN\frac{\partial N}{\partial \phi_0} - pw_1\frac{R}{2} = 0 \tag{7}$$

where

$$N = \frac{EA}{k\pi R}\left[w_1\phi_0 - w_0'\pi - \frac{\pi^2}{8R}\frac{w_1^2}{\phi_0}\right] \tag{8}$$

$$\frac{\partial N}{\partial w_1} = \frac{EA}{k\pi R}\left[\phi_0 - \frac{\pi^2}{4R}\frac{w_1}{\phi_0}\right]; \quad \frac{\partial N}{\partial \phi_0} = \frac{EA}{k\pi R}\left[w_1 + \frac{\pi^2}{8R}\left(\frac{w_1}{\phi_0}\right)^2\right] \tag{9a,b}$$

and for two lobe deformation prior to buckling:

$$k = 1, \quad w_0' = w_{02}, \quad C = \pi R/4EA, \tag{10}$$

whilst for single lobe behaviour prior to buckling:

$$k = 2, \quad w_0' = w_{01}, \quad C = \pi R/2EA, \tag{11}$$

and the generalised form of w_0' is $\int_0^{\pi D} w_0(s)\mathrm{d}s$.

Eqs. (6) and (7) constitute a set of non-linear simultaneous equilibrium equations relating the applied pressure to the deflection parameters w_1, ϕ_0 though the system properties E, I, A, R, w_0'. Thus, assuming that the system becomes geometrically unstable before material failure, Eqs. (6) and (7) provide the basis for determination of the following two critical situations:

(a) Buckling behaviour for systems possessing linear elastic material properties and subject to increasing load to failure, and
(b) Creep lives for systems with non-linear time dependent material properties and subject to constant (or gradually increasing) long-term loading.

3. Numerical determination of elastic buckling loads

The load-deflection path to failure can be obtained by incrementally increasing the applied load p and solving for the corresponding deflection parameters $w_1(p)$, $\phi_0(p)$ using Newton–Raphson iteration (Owen and Hinton, 1980). Thus at load p we seek the solution vector $\{x + \delta x\}$ to Eqs. (6) and (7), where $\{x\} = \{w_1, \phi_0\}^{\mathrm{T}}$, that satisfies the truncated Taylor series

$$f_i\{x + \delta x\} = f_i\{x\} + \sum_{j=1}^{2}\frac{\partial f_i}{\partial x_j}\delta x_j \tag{12}$$

Eqs. (12) reduce the original simultaneous non-linear equations (6) and (7) to a set of linear equations which move each function closer to zero simultaneously. At each load increment equations (12) are repeatedly updated until the solution for $\{x+\delta x\}$ has converged (Press et al., 1989). The required derivatives are obtained as:

$$\frac{\partial f_1}{\partial w_1}=\frac{\pi E}{8R^3}\left(\frac{\pi}{\varphi_0}\right)^3+\frac{EA}{2k\pi R}\left[\phi_0-\frac{\pi^2 w_1}{4\phi_0 R}\right]^2-\frac{EA}{2k\pi R}\left[\frac{\pi^2}{4\phi_0 R}\right]\left[w_1\phi_0-w_0'\pi-\frac{\pi^2 w_1}{8\phi_0 R}\right] \tag{13a}$$

$$\frac{\partial f_1}{\partial \phi_0}=-\frac{3EI}{8R^3}\left(\frac{\pi}{\phi_0}\right)^4 w_1+\frac{EA}{2k\pi R}\left[w_1\phi_0-w_0'\pi-\frac{\pi^2 w_1^2}{8\phi_0 R}\right]\left[1+\frac{1}{4}\left(\frac{\pi}{\phi_0}\right)^2\frac{w_1}{R}\right]$$
$$+\frac{EA}{2k\pi R}\left[w_1+\frac{1}{8}\left(\frac{\pi}{\phi_0}\right)^2\frac{w_1^2}{R}\right]\left[\phi_0-\frac{\pi^2 w_1}{4\phi_0 R}\right]-\frac{pR}{2} \tag{13b}$$

$$\frac{\partial f_2}{\partial w_1}=-\frac{3EI}{R^3}\left(\frac{\pi}{\phi_0}\right)^4 w_1+\frac{EA}{2k\pi R}\left[w_1\phi_0-w_0'\pi-\frac{\pi^2 w_1^2}{8\phi_0 R}\right]\left[1+\frac{1}{4}\left(\frac{\pi}{\phi_0}\right)^2\frac{w_1}{R}\right]$$
$$+\frac{EA}{2k\pi R}\left[\phi_0-\frac{\pi^2 w_1}{4\phi_0 R}\right]\left[w_1+\frac{1}{8}\left(\frac{\pi}{\phi_0}\right)^2\frac{w_1^2}{R}\right]-\frac{pR}{2} \tag{13c}$$

$$\frac{\partial f_2}{\partial \phi_0}=\frac{3EI}{4R^3}\frac{\pi^4}{\phi_0^5}w_1^2+\frac{EA}{2k\pi R}\left[w_1+\frac{1}{8}\left(\frac{\pi}{\phi_0}\right)^2\frac{w_1^2}{R}\right]^2-\frac{EA}{2k\pi R}\left[\frac{\pi^2 w_1^2}{4\phi_0^3 R}\right]\left[w_1\phi_0-w_0'\pi-\frac{\pi^2 w_1^2}{8\phi_0 R}\right] \tag{13d}$$

Eqs. (6), (7), and (13) are readily incorporated into a standard Newton–Raphson procedure (see e.g., Press et al., 1989) for the solution at specified load, and which can automatically be incremented for increasing load levels up to critical; k, C, and w_0' can be selected for one or two lobe buckling as appropriate. Fig. 4

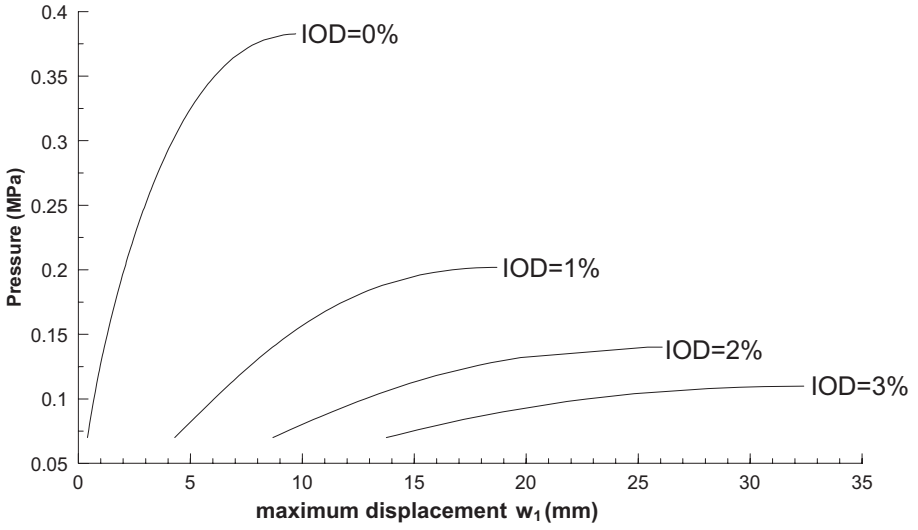

Fig. 4. Two lobe load deflection behaviour for a representative system (lining mean diameter = 450 mm, thickness = 6 mm, E = 3860 MPa) at imperfection on diameter (IOD) = 0%, 1%, 2%, 3%.

Table 1
Comparison of analytical and numerical solutions for a representative system ($D = 450$ mm, $t = 6$ mm, $E = 3860$ MPa)

Gap (%)	Analytical solution			Numerical solution
	c_1	c_2	P_{crit} (MPa)	P_{crit} (MPa)
0.0	−2.2	0.1215	0.383	0.383
0.5	−2.705	0.786	0.202	0.202
1.0	−2.856	0.919	0.140	0.140
1.5	−2.896	0.888	0.110	0.110
2.0	−2.930	0.870	0.0918	0.0918

shows the results obtained for a representative system (lining diameter $D = 2R$, lining thickness t) at a range of imperfections, and where:

$$\text{IOD} = \text{imperfection on diameter} = 2w_{02}/D$$

Thus w_0 is taken to be in the form of a symmetrical gap (see Fig. 1a) with the deformation mode as shown in Fig. 1b. Each curve represents the load-deformation trace up to the maximum sustainable pressure (p_{crit}) at which point the analysis becomes numerically unstable. Boot (1998) has shown how Eqs. (6) and (7) can be solved analytically to yield p_{crit} under these conditions. The solution can be specified at any gap in the general form:

$$\log\left(\frac{p_{crit}}{E}\right) = c_1 \log\left(\frac{D}{t}\right) + c_2 \tag{14}$$

The results obtained from Fig. 4 and Eq. (14) are compared in Table 1, and are identical to three significant figures, thus verifying the proposed numerical procedure.

4. Creep life determination under constant long-term pressure loading

The linear elastic situation investigated in the previous section is representative of a short-term laboratory test to failure under increasing load, using a typical commercial thermosetting polymeric lining (Boot and Javadi, 1998a). However, as described in Section 1, the long-term design criterion for a nominally circular polymeric lining is constrained creep buckling. The solution to Eqs. (6) and (7) at any pressure p can be written in the form:

$$\{w_1, \phi_0\} = f\left(\frac{t}{R}, \frac{w_0}{R}, \frac{p}{E}\right) \tag{15}$$

The extension of time independent to time dependent (creep) buckling is a classical problem (Kollár and Dulácska, 1984; Godoy, 1996). Under constant or gradually increasing loads there are no inertia effects and the equations for a static solution remain valid provided the revised material properties can be suitably defined. For the problem under consideration we deem the creep pressure loading to be applied over a short period (generating an initial linear elastic response) and subsequently held constant over the creep life. Then since t, R, w_0, p are not functions of time (τ), when solving Eq. (15) for creep behaviour we seek the solution for increasing $\{w_1, \phi_0\}$ with time as $E(\tau)$ decreases. Therefore, the numerical solution of Eqs. (6) and (7) described in Section 3 can be amended to solve for creep buckling lives using a time stepping procedure (Owen and Hinton, 1980) provided $E(\tau)$ for the lining material can be suitably defined.

A series of uniaxial flexural and compressive creep tests has been undertaken over a range of constant working stress levels (Boot and Welch, 1989; Javadi and Boot, 1998) using a particular reinforced polyester

Table 2
Power law parameters defining Eq. (16) for a commercial pipelining material

Stress state	m	n	A (MPa$^{-m}\tau^{-n}$)
Flexure	1.115	0.064	2.360×10^{-4}
Compression	0.906	0.079	2.904×10^{-4}

resin typical of those used for CIPP close-fitting sewer linings. The results exhibited constitutive behaviour expressible in the form:

$$\varepsilon(\sigma,\tau) = A\sigma^m\tau^n \tag{16}$$

The values of the parameters obtained are given in Table 2, and indicate a significantly stiffer response in compression than tension, possibly due to a microfracture deformation mechanism.

Eq. (16) is an empirical fit to constant stress creep data, and represents the unique relationship between stress and strain observed under the constant stress states investigated. This total strain theory is therefore a non-linear elastic formulation, and not valid under generalised loading conditions (Hult, 1966). However, since the problem under investigation does not involve unloading, and there is only a very gradual increase in stress with time as axial–flexural interaction progresses, this concept should provide an adequate constitutive model for present purposes.

For non-linear elasticity Eqs. (4) are usually taken (see eg. Zhu and Hall, 2001) to define E as the instantaneous secant modulus $E_S(\sigma,\tau)$ as shown in Fig. 5. This definition is valid provided the elasticity equations are only mildly non-linear (Boot and Welch, 1996). $E_S(\sigma,\tau)$ can be obtained from Eq. (16) via its inverse as:

$$\frac{1}{E_S(\sigma,\tau)} = \frac{\varepsilon(\tau)}{\sigma(\tau)} = A\sigma^{(m-1)}\tau^n \tag{17}$$

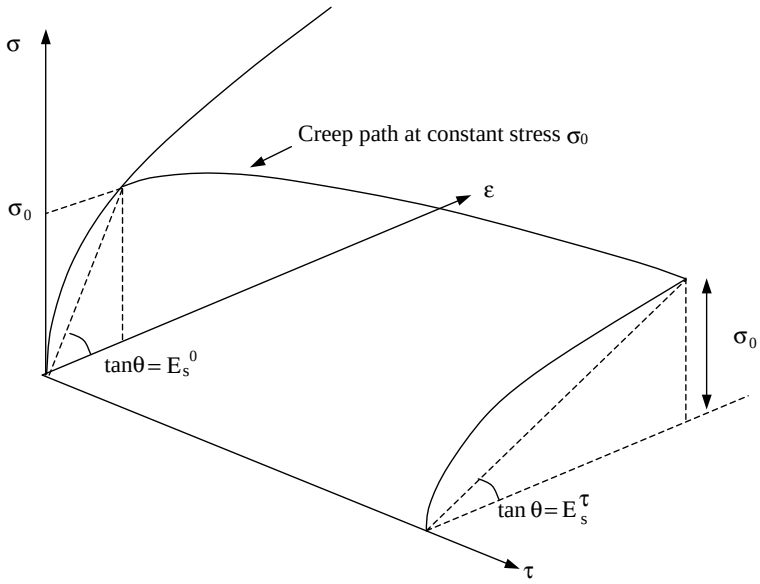

Fig. 5. Illustrating initial (E_S^0) and general (E_S^t) secant moduli at a constant creep stress σ_0.

The non-linear elastic extension of Eqs. (6) and (7) can now be expressed in the form

$$f_i(x_1, x_2, \tau) = 0 = E_S(\sigma, \tau) f_i'(x_1, x_2) - \frac{pR}{2} x_i \tag{18}$$

where $i = 1, 2$ in turn, x_1, $x_2 = w_1$, ϕ_0, and f_i' are defined by equivalence of Eqs. (6), (7) and (18). Similarly the solution to Eqs. (18) at time $t + \delta t$ becomes

$$f_i(x_1 + \delta x_1, x_2 + \delta x_2, \tau + \delta\tau) = E_S(\tau + \delta\tau) f_i'(x_1 + \delta x_1, x_2 + \delta x_2) - \frac{pR}{2}(x_i + \delta x_i) \tag{19}$$

The first term on the right hand side of Eqs. (18) and (19) is separable in τ and x_1, x_2. Furthermore, the value of $E_S(\tau + \delta\tau)$ can be written from Eq. (17) as

$$\frac{1}{E_S(\sigma, \tau + \delta\tau)} = \frac{\varepsilon(\tau + \delta\tau)}{\sigma(\tau + \delta\tau)} = A\sigma(\tau + \delta\tau)^{(m-1)}(\tau + \delta\tau)^n$$

Once $E_S(\sigma, \tau + \delta\tau)$ is explicitly defined, Eqs. (19) revert to the form of Eqs. (6) and (7), and can therefore be solved in exactly the same way. Now initially we use the explicit prediction $\sigma(\tau + \delta\tau) = \sigma(\tau)$ to obtain $E_S(\tau + \delta\tau)$ in Eqs. (19) and successively update $\sigma(\tau + \delta\tau)$ until E_S has converged (see e.g., Owen and Hinton, 1980).

Finally it is necessary to identify a means of utilising the different responses obtained in compression and flexure, noting that the actual condition generated in a gravity pipe lining is a combination of these two stress states. In this respect, provided failure is due to buckling rather than material breakdown, the effect of superimposing a state of compression on a microfracturing material is to close the cracks and enhance performance. This suggests a response intermediate between those defined by the individual stress states is implied over the stress range of interest. Furthermore, since Table 2 shows that the spread in the values of corresponding material parameters is no more than 20%, we assume that all consistently defined variations in constitutive behaviour between the two stress states will give essentially similar results. Accordingly we here consider, as a first approximation, the simplest such model:

$$\sigma = E_{SA}\varepsilon_A + E_{SB}\varepsilon_B \tag{20}$$

where σ is the extreme fibre total stress and:

$$E_{SB} = \left[A_B \sigma^{(m_B - 1)} \tau^{n_B}\right]^{-1}; \quad E_{SA} = \left[A_A \sigma^{(m_A - 1)} \tau^{n_A}\right]^{-1} \tag{21a; 21b}$$

In Eqs. (20) and (21) the subscripts B and A indicate material constants obtained in bending and axial compression respectively, as defined in Table 2. Substituting Eqs. (21) into Eqs. (4), (6), (7), and (13) results in essentially unmodified equations with EI, EA replaced everywhere by $E_{SB}I$, $E_{SA}A$ respectively.

In the proposed numerical analysis material properties are evaluated at the location of maximum deflection (w_1), which is the cross-section carrying the maximum tensile and compressive strains in the lining. The stresses at all other cross-sections are then defined by these values of E_{SB}, E_{SA} and Eqs. (3) and (4). Since $m \approx 1$, this will render an otherwise slightly over-stiff solution a little more flexible, and should not therefore imply any significant additional approximation.

The flow diagram delineated in Fig. 6 illustrates the major steps in the solution process. At step 1 input of the system geometric and material parameters is required. Fig. 7 illustrates the basic creep performance at constant stress. Eq. (16) represents only the primary and secondary creep response; an independent initial elastic modulus can be defined using standard short-term testing procedure. This can be used to obtain the linear elastic solution at $\tau = 0$, with the full load (p) applied at this stage (Fig. 7, point A). The creep process can then be started from $\tau = 1$ h (Fig. 7, point B). An initial approximation (w_1, ϕ_0) is therefore required at step 2, from which the linearly elastic solution at $\tau = 0$ can converge. This can be obtained by establishing p_{crit} for this system using Eq. (14) and the identified short-term modulus. Thence the value of w_1

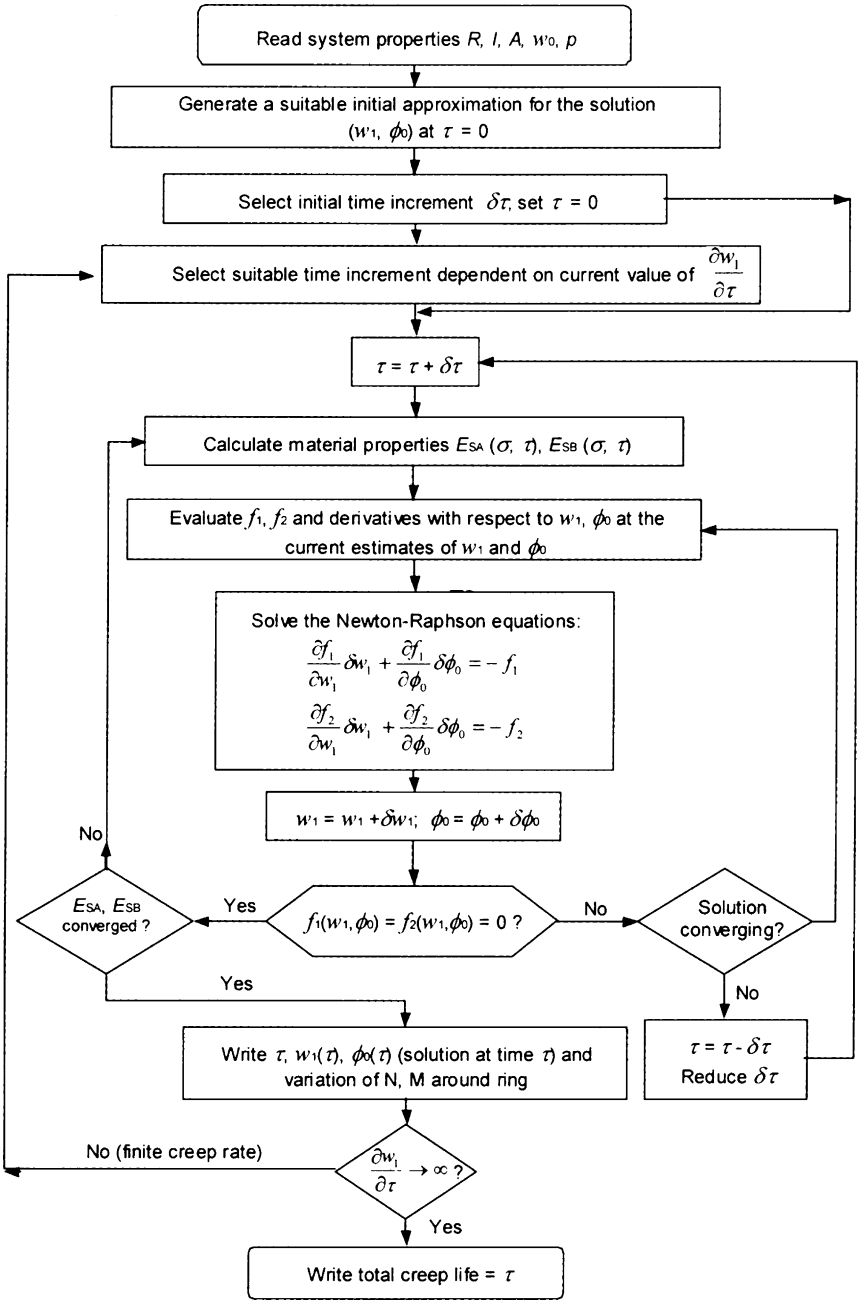

Fig. 6. Flow chart for the creep solution process described in Section 4.

corresponding to p_{crit} can be obtained and proportioned by p/p_{crit}. The value of w_1 so calculated can be taken with any reasonable value for ϕ_0 (say 5–45°, see Fig. 3) to provide appropriate starting values.

At step 3 set $\delta\tau = 1$ h, $\tau = 0$; steps 6–9 and corresponding convergence criteria then obtain the initial creep solution at $\tau = 1$ h by Newton–Raphson iteration (Press et al., 1989). $\delta\tau$ is retained at 1 h for the first

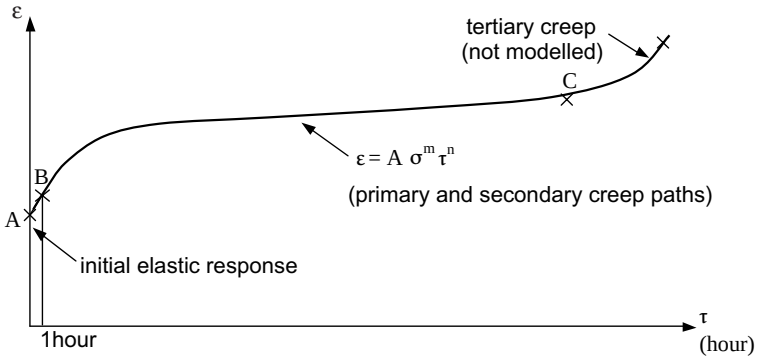

Fig. 7. The basic material creep process for (approximately) constant stress and its numerical implementation.

increment of creep deformation, and subsequently redefined as appropriate to follow the creep process, taking this to be controlled by secondary creep of the lining material throughout the vast majority of the system life. Thus secondary material creep will eventually precipitate tertiary system creep due to the increasing bending moments generated by the constant axial hoop force acting at increasing eccentricity due to the accumulating creep deformations. Creep buckling can be sensibly taken to occur at the onset of tertiary system creep (Fig. 7, point C) as this is a reasonably clearly defined point beyond which creep life is relatively short and unstable. Fig. 8 shows the creep response obtained by the proposed simple solution for a typical problem with the following specification:

Outside lining diameter (D_e) = 300 mm
Lining thickness (t) = 6 mm
SDR = $D_e/t = 50$
Symmetrical gap (w_{02}) = 1.4 mm (0.467%)
E (lining) defined by the flexural creep properties given in Table 2 and a short-term value of 3860 MPa.

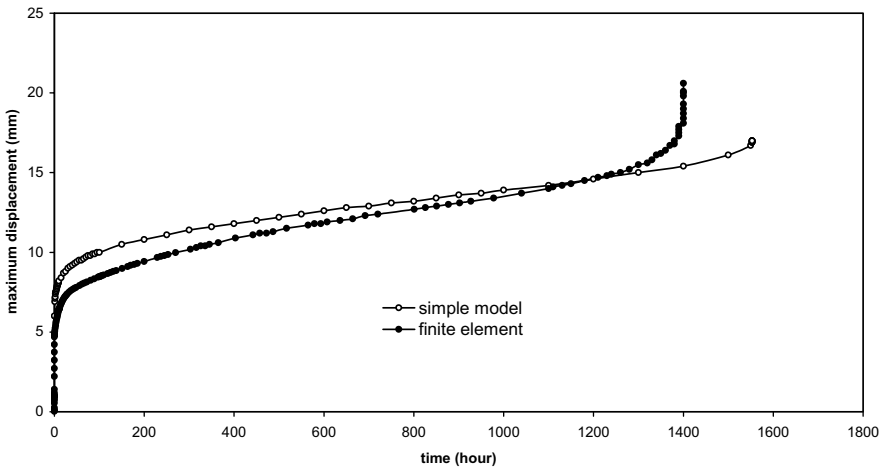

Fig. 8. Comparison of creep curves obtained from the simple model and FE analysis for the representative problem specified in Section 4.

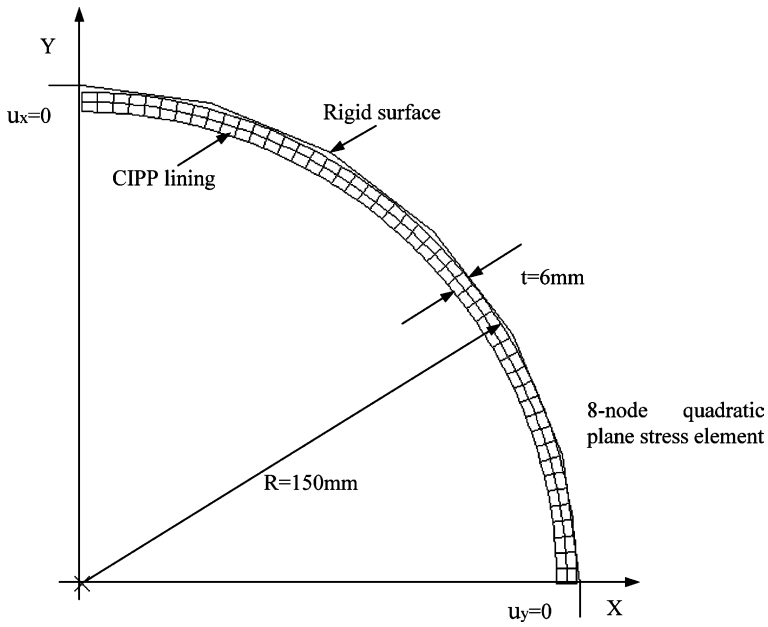

Fig. 9. FE model used to simulate two lobe creep buckling.

Also shown is the corresponding result obtained from a FE analysis of the same problem (Abaqus 5.8, 1998). The major details of the FE simulation are illustrated in Fig. 9; only one quadrant is modelled due to symmetry. For single lobe behaviour, two quadrants are modelled, and the rigid surface located eccentric to the lining (i.e., contact at one point). The FE simulation incorporates a viscoelastic representation of the same creep data (Poisson's ratio $v = 0.37$) of the form:

$$\sigma_{21} = \int_0^{\tau} G(\tau - \tau')\dot{\gamma}_{21}(\tau')\,\mathrm{d}\tau'$$

where σ_{21}, $\dot{\gamma}_{21}$ are shear stress and strain rate, G is the 'relaxation modulus', and the integration is carried out over all past times τ' up to the current time τ. $G(\tau)$ is obtained from the best least squares fit to the extreme fibre strain–time data from the uniaxial flexural tests (Ferry, 1980).

There are therefore significant differences between the two analyses:

- The material models used are different 'best fits' to the data; in particular $G(\tau)$ is the same at all stress levels (equivalent to $m = 1$).
- The FE simulation is a fully geometrically non-linear two-dimensional plane stress analysis and a consistent contact algorithm is defined at the correct location, whereas the simple analysis is a centroidal model.
- The time-stepping procedures are different.

Nevertheless, these significant differences in formulation result only in minor differences in overall behaviour as illustrated in Fig. 8, which demonstrates the mutually supportive nature of both sets of results. However, the FE analysis is not suitable for routine design, and cannot take account of the different properties measured in flexure and compression for the representative material.

Fig. 10 shows the test data obtained from a set of physical creep tests (in which linings were subject to external pressure), together with numerical predictions for these results obtained using the analysis of Fig. 6

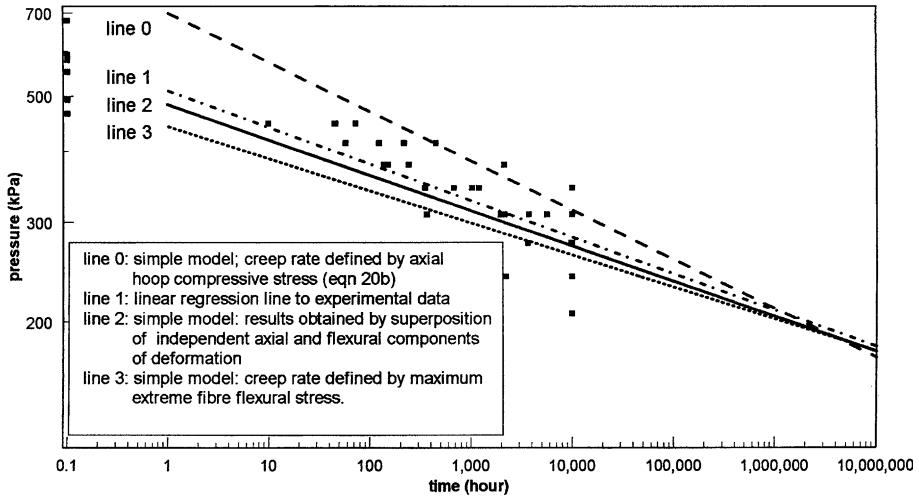

Fig. 10. Comparison of simple model and FE results with the experimental data due to Guice et al.

incorporating the material properties specified by Eqs. (16), (20) and Table 2. The physical test results are those reported by Guice et al. (1994). The linings were of 300 mm external diameter, 6 mm thickness, and were tested as cast—i.e., incorporating a small approximately symmetrical gap with the host pipe caused by curing shrinkage. The following points are pertinent to the interpretation of this data:

(a) The linings were made of essentially the same material as that quantified by Eq. (16) and Table 2. Guice et al. did not directly assess material creep. Nevertheless, since both measurements of short-term flexural properties yielded very similar results, it can be reasonably assumed that long-term mechanical response in the creep pressure tests of Guice et al. can be defined by Eq. (16) and Table 2.
(b) Failure in all cases was reported to be due to geometrical instability (creep buckling) rather than material breakdown.
(c) No deformations were monitored in these tests. Nevertheless, subsequent test monitoring using the same basic test technique at the same laboratory (Seeman et al., 2001; Zhu and Hall, 2001) strongly suggests that these samples all experienced two lobe deformation prior to buckling. This is also in agreement with similar test results obtained by others (Boot and Welch, 1996). Accordingly numerical predictions of Guice et al.'s results are here obtained using k, w_0', C defined according to Eqs. (10).
(d) Study of Eq. 14 and Table 1 shows that up to $w_{02} \approx 0.7\%$, system behaviour is imperfection sensitive, with p_{crit} decreasing in a non-linear manner as w_{02} increases. Conversely for $w_{02} \geqslant 1\%$ p_{crit} decreases approximately linearly with w_{02} over the range of w_{02} of practical interest. Guice et al. approximately assessed the initial gaps in their systems by measuring the *maximum* gap at each end of every test specimen using a ruler. These results yield an overall average *maximum* gap for all 37 specimens in the test series of $0.77 \pm 0.41\%$ (mean $\pm$ standard error in mean). Thus we conclude that a proportion of these tests will have exhibited imperfection sensitive behaviour, and this fact has no doubt contributed to the level of scatter in the results obtained.
(e) Nevertheless, every effort was made to maintain homogeneity of lining properties and test procedure for all specimens, and the results demonstrate typical spreads for creep testing of one logarithmic decade in time at each test pressure. Accordingly the discrepancies from mean behaviour can be anticipated to be distributed at random in a statistically valid manner. Since creep behaviour is essentially a power law (logarithmic) function of the system parameters (Struik, 1978) the linear regression line

though the creep life/pressure data in logarithmic space (Line 1, Fig. 10) can therefore be expected to provide a comparable estimate of performance in the mean to that predicted by a valid mathematical model incorporating the average measured system properties.

Based on the above observations, we conclude that these results can be used to establish the validity of the proposed numerical and material modelling procedures. The numerical results presented in Fig. 10 assume a symmetrical annular gap imperfection of 1.4 mm or 0.952% IOD. This is slightly greater than the average measured gap, but within the range, measured by Guice et al. However, it must be recalled that their measurement of gap was only local and approximate. Furthermore, in addition to the gap, there will also be imperfections in lining thickness, material property, and circularity. If all the imperfections in the system are considered to contribute to an equivalent *characteristic gap* imperfection (i.e., *characteristic* of the system under consideration) this will clearly be slightly higher than the actual average gap.

Line 0 shows the creep life against time relationship predicted by the numerical analysis incorporating the axial compressive creep data. As might be expected, this material model yields a significant upper bound to the creep buckling data, since the flexural component of strain is underestimated. In addition, the slope of this line is clearly greater than that of the regression line. It has been argued that a better use of the overall available creep data is superposition of the independently measured axial and flexural components of deformation according to Eqs. (20), (21), and Table 2. Line 2 shows that the solution obtained using this material model compares extremely well with the test data regression line. Nevertheless, this is a very inconvenient material model for design purposes, since it requires two sets of creep tests to be undertaken for any given material. In particular, current design focuses on the flexural creep properties (WIS 4-34-04, 1995; ASTM F 1216-98), and it is therefore of interest to investigate the level of approximation implied by this procedure. Line 3 shows the solution obtained using the flexural modulus (obtained from Eq. (16) and Table 2) corresponding to the extreme fibre flexural stress at the cross-section experiencing maximum deflection. This is also a remarkably close approximation to the regression line though the experimental data, and gives an almost identical solution to the FE model (not plotted to avoid confusion).

Clearly, the significance of the results presented in Fig. 10 depends to some extent on the validity of the assumed symmetrical gap imperfection of 1.4 mm. Fig. 11 shows that the slope of the prediction line is

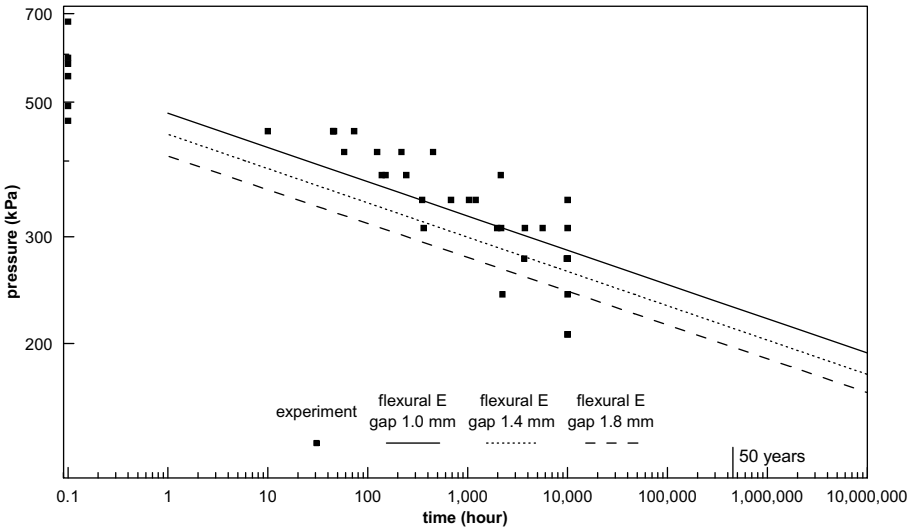

Fig. 11. Showing the effect of varying initial gap on the solution given by line 3 on Fig. 10.

unaffected by variation in gap, but that the intercept is quite sensitive to this parameter. In addition the most appropriate characteristic gap imperfection to adopt for this system can only be identified by means of back-analysis and statistical examination using the available test data. In this respect the value adopted of $w_{02} = 1.4$ mm ($\approx$1% of pipe radius), is consistent with all the measurements and qualitative arguments governing selection of this parameter. Furthermore, the simple solution procedure incorporating the material formulation based on superposition of the flexural and axial compressive creep data (Eqs. (20), (21) and Table 2) and the linear regression line to the physical data show a level of agreement well within the statistical validity of the latter.

5. Conclusions

1. Design of nominally circular polymeric linings for gravity pipes requires a determination of creep life subject to constant external hydrostatic pressure.
2. Providing an adequate safety factor against constrained creep buckling of the lining within the rigid constraint of the host pipe–soil system is normally the critical design criterion for the thin-walled linings used for this purpose.
3. The stress state in the lining is therefore one of combined bending and membrane compressive stresses. Standard creep testing of a representative polymeric material under pure bending and axial loading has revealed significantly different responses in the two stress states. Both physical and numerical test data indicates these systems fail in geometric instability prior to any material yielding or fracture.
4. An existing relatively simple analysis for the determination of linearly elastic buckling pressures for circular linings subject to small imperfections has here been re-expressed in a more generalised non-linear elastic form, including independent response in flexure and compression, to more closely simulate the observed material behaviour. The equations have then been expressed in a form suitable for numerical solution, and a simple time-stepping procedure for determination of creep lives based on the onset of buckling has been developed. The results obtained have been verified against corresponding FE and physical test results. The simple analysis has therefore been shown to give a convenient solution to the problem posed.
5. In addition it has been shown that for the material investigated, the simple analysis defined in terms of the time-dependent non-linear elastic modulus obtained in pure flexure gives a very good correlation with the test data, and consequently there is no significant advantage in using the more complex formulation incorporating separate moduli for the flexural and compressive deformations. This observation amounts to an endorsement of current (previously unvalidated) industrial procedure.

Acknowledgements

The Authors acknowledge the financial and technical support for the work reported here of the Engineering and Physical Sciences Research Council (UK) and Insituform Technologies Inc. In particular our thanks go to Dr. J.E. Gumbel of Insituform for his continual support and guidance.

References

Abaqus Documentation: Version 5.8 (1998), Hibbitt, Karlsson and Sorenson Inc., Rhode Island, USA.

Amstutz, E., 1969. Das Einbuelen von Schacht und Stollenpanzerungen, Schweizerische Bauzeitung, 87, 541-549, United States Department of the Interior, Bureau of Reclamation, Translation no. 826.

ASTM F 1216 98 1998. Standard practice for rehabilitation of existing pipelines and conduits by the inversion and curing of a resin-impregnated tube. American Society for Testing and Materials, Philadelphia.

Boot, J.C., 1998. Elastic buckling of cylindrical pipe linings with small imperfections subject to internal pressure. Trenchless Technology Research 12, 3–15.

Boot, J.C., Welch, A.J., 1989. Establishing and implementing the long term constitutive behaviour of structural plastic pipe linings. In: Armer, G.S.T., Clarke, J.L., Garras, F.K. (Eds.), The Life of Structures. Butterworths, London, pp. 283–290.

Boot, J.C., Welch, A.J., 1996. Creep buckling of thin-walled polymeric pipe linings subject to external ground water pressure. International Journal for Thin-Walled Structures 24, 191–210.

Boot, J.C., Javadi, A.A., 1998a. Experimental determination of buckling capacities for cured-in-place pipe linings. In: Allinson, I.M. (Ed.), Proceedings of 11th International Conference on Experimental Mechanics, Oxford, August, 1998. Balkema, Rotterdam, pp. 327–332.

Boot, J.C., Javadi, A.A., 1998b. The structural behaviour of cured-in-place pipe linings, Plastics Pipes X. In: Proceedings of Conference, Gothenberg, September 1998, pp. 369–378.

Boot, J.C., Toropova, I.L., Ashour, A.F., 2001. The structural performance of flexible sewer linings subject to external pressure. In: Knight, M., Thompson, N. (Eds.), Underground Infrastructure Research. Balkema, Lisse, pp. 39–47.

El-Sawy, K.,Moore, I.D., 1997. Parametric study for buckling of liners: effect of liner geometry and imperfections, trenchless pipeline projects: practical applications. In: Osborn, L. (Ed.), Proceedings of ASCE Pipelines Division Conference held in Boston, MA. ASCE, pp. 416–423.

Ferry, J.D., 1980. Viscoelastic Properties of Polymers. Wiley, New York.

Glock, D., 1977. Überkritisches Verhalten einees starrr ummantelten Kreisrohes bei Wasserdruck von aufen und Temperaturdehnung, Der Stahlbau, vol. 7, pp. 212–217.

Godoy, L.A., 1996. Thin-Walled Structures with Structural Imperfections. Elsevier, Oxford.

Guice, L.K., Straughn, W.T., Norris, C.R., Bennett, R.D., 1994. Long-term structural behaviour of pipeline rehabilitation systems, Technical Report no. 302, Trenchless Technology Centre, Louisiana Technical University, Ruston, Louisiana, USA.

Gumbel, J.E., 1997. Structural design of pipe linings review of principles, practice and current developments worldwide, No-Dig 97, Proceedings of Conference, Taipei, Taiwan, 1997.

Gumbel, J.E., 2001. New approach to design of circular liner pipe to resist external hydrostatic pressure. In: Joseph, P. (Ed.), Advances in Pipeline Engineering and Construction, Proceedings of ASCE Pipelines Division Conference held in San Diego, CA, Castronovo, ASCE.

Hult, J.A.H, 1966. Creep in Engineering Structures. Blaisdell, Waltham, MA, USA.

Javadi, A.A., Boot, J.C., 1998. Material testing of CIPP pipe linings: detailed procedures, results and analysis, Civil Engineering Research Report no. 56, School of Engineering, University of Bradford, Bradford, UK.

Kollár, L., Dulácska, E., 1984. Buckling of Shells for Engineers. Wiley, New York.

Moore, I.D., 1998. Tests for liner stability: what we can and cannot learn. In: Proceedings of North American No-Dig '98 Conference, Albuquerque, NM, North American Society for Trenchless Technology.

Omara, A.M., Guice, L.K., Straughan, W.T., Akl, F.A., 1997. Buckling models of thin circular pipes encased in rigid cavity. Proceedings of the ASCE, Journal of Engineering Mechanics 123, 1294–1301.

Owen, D.R.J., Hinton, E., 1980. Finite Elements in Plasticity. Pineridge Press, Swansea, UK.

Press, W.H., Flannery, B.P., Teukolsky, S.A., Vetterling, W.T., 1989. Numerical Recipes. Cambridge University Press, Cambridge, UK.

Seeman, R., Hall, D.E., Straughan, W.T., 2001. Buckling experiments for CIPP liners installed in ovalised host pipes. Technical Report no. 2001.04, Trenchless Technology Centre, Louisiana Technical University, Ruston, Louisiana, USA.

Struik, L.C.E., 1978. Physical Aging in Amorphous Polymers and Other Materials. Elsevier, Amsterdam.

Toropova, I.L., Boot, J.C., 1998. Mathematical modelling of buckling capacities of cured-in-place pipe for sewer linings, Civil Engineering Research Report no. 59, School of Engineering, University of Bradford, Bradford, UK.

Washizu, K., 1982. Variational Methods in Elasticity and Plasticity, third ed. Pergamon Press, Oxford.

Weaver, R., De Rosa, J., Ovington, S., 1999. Renovation using deformed PE Liners Subline: a novel close-fit thin-wall PE lining technology. In: Rehabilitation: Piping and Infrastructure Conference, University of Newcastle, March 1999.

WIS 4-34-04, 1995. Specification for renovation of gravity sewers by lining with cured-in-place pipes, WRc Engineering, Swindon, UK.

WRc Engineering, 1995. Sewerage Rehabilitation Manual, WRc Engineering, Swindon.

Yamamoto, Y., Matsubara, N., 1981. Buckling strength of steel cylindrical liners for waterway tunnels. Theoretical and Applied Mechanics 30, 225–235.

Zhu, M., Hall, D.E., 2001. Creep induced contact and stress evolution in thin-walled pipe liners. International Journal for Thin-Walled Structures 39, 939–959.